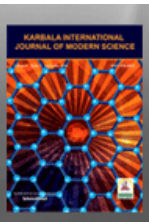

Karbala International Journal of Modern Science

Volume 8 | Issue 2 Article 15

Simulating photo-disintegration of 137Cs radioactive waste using various energies of gamma photons

Hassanain H. Alkazzaz
Ph.D. student, Department of physics, collage of science, University of Baghdad., h.h.alkazzaz.phys@gmail.com

Asia H. Al-Mashhadani
Department of physics, collage of science, University of Baghdad.

Kamal H. Lateef
Chairman of Iraqi Radioactive Sources Regulatory Authority, Baghdad, Iraq

Recommended Citation

Alkazzaz, Hassanain H.; Al-Mashhadani, Asia H.; and Lateef, Kamal H. (2022) "Simulating photo-disintegration of 137Cs radioactive waste using various energies of gamma photons," *Karbala International Journal of Modern Science*: Vol. 8 : Iss. 2 , Article 15.
Available at: https://doi.org/10.33640/2405-609X.3230

Simulating photo-disintegration of 137Cs radioactive waste using various energies of gamma photons

Abstract

In this study, the possibility of using gamma-ray in photo-disintegration method was examined so that it can be used in the remediation of 137Cs radionuclides waste materials by nuclear transmutation to convert long-lived nuclides to other isotopes nuclides, which are shorter half-life (or stable), by different photo-nuclear reaction channels (γ,n), (γ,2n), (γ,p), (γ, a), (γ,d). A simulation code has been written using MATLAB for conducting calculations of reduction and residual. The results showed that gamma-ray fluxes below 1017 [cm-2 s-1] are not adequate to perform effective incinera-tion of 137Cs, and as for gamma flux of 1018 [cm-2 s-1] it showed that it provides incineration rate of about 100 times faster than the natural decay of cesium 137. This paper also shows that the recommended range of incineration photons energy Eγ should be between 8.27

Keywords

photo-disintegration, nuclear transmutation, waste treatment, 137Cs, gamma incineration

RESEARCH PAPER

Simulating photo-disintegration of ^{137}Cs radioactive waste using various energies of gamma photons

Hassanain H. Alkazzaz [a,*], Asia H. Al-Mashhadani [a], Kamal H. Lateef [b]

[a] Department of Physics, College of Science, University of Baghdad, Iraq
[b] Chairman of Iraqi Radioactive Sources Regulatory Authority, Baghdad, Iraq

Abstract

In this study, the possibility of using gamma-ray in photo-disintegration method was examined so that it can be used in the remediation of ^{137}Cs radionuclides waste materials by nuclear transmutation to convert long-lived nuclides to other isotopes nuclides, which are shorter half-life (or stable), by different photo-nuclear reaction channels (γ,n), (γ,2n), (γ,p), (γ, a), (γ,d). A simulation code has been written using MATLAB for conducting calculations of reduction and residual. The results showed that gamma-ray fluxes below 10^{17} [cm^{-2} s^{-1}] are not adequate to perform effective incineration of ^{137}Cs, and as for gamma flux of 10^{18} [cm^{-2} s^{-1}] it showed that it provides incineration rate of about 100 times faster than the natural decay of cesium 137. This paper also shows that the recommended range of incineration photons energy E_γ should be between 8.27<E_γ<15.1 MeV.

Keywords: Photo-disintegration, Nuclear transmutation, Waste treatment, ^{137}Cs, Gamma incineration

1. Introduction

One of the primary issues concerning the management of hazardous radioactive waste is the disposal of high-level radioactive waste including long-lived nuclides such as 137Cs.

The International Atomic Energy Agency divides radioactive waste into six groups (categories), which are based on the activity and half-life of radionuclides [1] as follows (from low to high hazardous):

- Exempted waste.
- Very short-lived waste.
- Very low-level waste.
- Low-level waste.
- Intermediate-level waste.
- High-level waste.

In general, the typical process of management of radioactive waste can be summarized by the sequent steps [2]: **Pretreatment**: Which involves the collection of waste, characterization, segregation, adjustment and decontamination. **Treatment**: The principal goals of treatment are to reduce volume, remove radionuclides from waste, and modify the physical and chemical composition. **Conditioning**: In this stage, a waste package is produced ready to be handled, transported or disposed. It may include solidification, embedding, encapsulation followed by packaging. **Interim storage**: Where radioactive waste is stored in a nuclear plant under human supervision and retrievability. **Transport**: The waste packages are transferred to a disposal site. And finally the **Disposal**: It is done according to the half-life of the radioactive waste where a deep underground repository is chosen for radio-nuclides of half-lives > 30 years or near-surface repository for shorter half-lives radionuclides.

As a result of previous nuclear activities in Iraq, there is a bulk of ^{137}Cs contaminated water in the pool of reactor, in addition to a great number of unused ^{137}Cs radioactive sealed sources which are stored in a storage bunker (Bunker B) in Twaitha site south of Baghdad. Also, there is a huge amount of ^{137}Cs contaminated soil stored in drums inside a warehouse in the site. All of these need to be treated

Received 7 January 2022; revised 2 April 2022; accepted 3 April 2022.
Available online 1 May 2022.

* Corresponding author at:
E-mail addresses: h.h.alkazzaz.phys@gmail.com (H.H. Alkazzaz), assia19662006@yahoo.com (A.H. Al-Mashhadani), kamalhlatif@yahoo.com (K.H. Lateef).

https://doi.org/10.33640/2405-609X.3230

and managed to reduce hazards and to protect the environment.

Short-lived radionuclides wastes are easy to manage as they decay to stable nuclides within a short time of storage. Whereas the long-lived radioactive waste needs special methods of treatment. In the current paper, a non-traditional manner in treatment by transmutating the long-lived radioactive waste into short-lived or stable nuclides is suggested as a promising manner to resolve the radioactive waste problem [3].

This method is summarized as a nuclear reaction induced by high energy gamma photons of energies sufficient to achieve reaction. Therefore, photons of energies greater than photo-nuclear reaction threshold energy are required and within the giant dipole resonance energy band. The advantages of using photo-nuclear transmutation are a broadened distribution of photo-absorption (non-elastic) cross-section which gives partial width Γ of an order of MeVs compared with neutron transmutation which has a partial width of capture Γ of an order of few eVs. On the other hand, the disadvantage of using the photo-nuclear transmutation method is the relatively low absorption cross-section value (with an order of millibarn), while for neutron capture the cross-section is much higher (with an order of hundreds of barn).

This method have been studied in literature; Matsumoto [4] proposed a gamma-ray method using photo-nuclear reactions for the degradation of 90Sr and 137Cs. High energies (10−20 MeV) gamma − photons, that would effectively be generated by an electron linear accelerator, by interacting with most nuclei through the (giant resonance) photo-nuclear cross-sections. Berman [5] exhibited photo-neutron cross-section data that were obtained using mono-energetic gamma photons. Swanson [6] calculated the yields of low-energy neutrons released by electrons incident on selected materials. Saeed [7] investigated the (γ − n) reaction cross-section for some radioactive fission products. Takai and Hagino [8] have quantitatively studied the effectiveness of the degradation with laser Compton scattering based on the Hauser − Feshbach theory. TALYS code has been used in their calculations. They ran simulations for the high-decay rate nuclide Cesium-137, calculating the (γ, γ), (γ, n), and (γ, 2n) cross-sections for the 137Cs and overall photo-nuclear reaction cross-sections versus input photon energy. They discovered that transmuting 137Cs with a medium-energy gamma photon flux larger than 1018 [cm^{-2} s^{-1}] efficiently decreases the target's radioactivity.

2. Source of high energy photons

High-energy photons with energy between 10 and 20 MeV that can be generated easily by an electron linear accelerator, interact with most nuclei through the giant resonance of photo-nuclear cross-sections. Medical linear accelerator (LINAC) is a good example of electron/photon generating machines. This machine is widely used in clinical centers around the world for therapeutics purposes, it generates a photon flux of the order 10^{10}-10^{12} [cm^{-2} s^{-1}].

Laser-Compton Scattering (LCS) is the latest method to generate a quasi-monochromatic and polarized gamma-ray beam. When laser photons of energy 0.7 eV (infrared laser) collide with relativistic electrons (of 1.2 GeV energy), the incident photon is scattered by the relativistic electron. The scattered photon energy is converted to a gamma-ray [9], as shown in Fig. 1.

3. Photon fluence calculation

Medical LINAC is a dependable source of high-energy photons. They use non-conservative microwave RF waves ranging from 10^3 MHz to 10^4 MHz (the majority operating at 2856 MHz), to accelerate electrons to kinetic energies of 4−25 MeV.

LINAC are composed of an electron gun, which is a heated filament conductor that generates electrons, accelerating wave guide generated from high intensity microwave source (Klystron or Magnetron), beam bending magnets for bending and focusing the electron beam on the tungsten target which is located in the upper position of the treatment head [10].

The energy spectra of clinical LINAC was studied by Mohan et al. [11]. They evaluated the spectra of

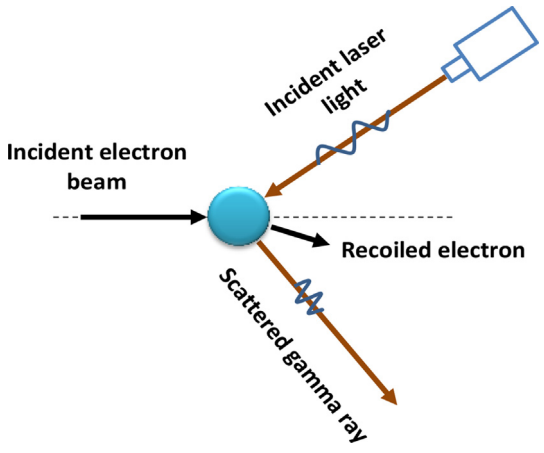

Fig. 1. Schematic of photon-electron collision and scattered gamma photon generated.

15 MV of Clinac-20 for axial beam and angular distance of 10–15 cm on the SSD surface (source to surface distance) using Monte Carlo code (EGS). They found that the average photon energy has a value lower than the generally perceived value of 1:3 of the maximum energy, also they found that the photon spectra becomes softer as the distance from central axis increases. Sheikh-bagheri and Rogers [12,13] investigated the simulation of spectra and average energy distributions of 9 MV selected using BEAM code and they compared their results with Mohan et al. results [11].

Brualla et al. [14] employed the (EGS4)/(BEAM) Monte Carlo code to examine the photon spectra, however, they found considerable differences with the most commonly used photon data set. They examined 4 MV (widely used in medical therapy) of Varian LINAC 6, 10, 15 & 20 MeV. In the current work, we used the same distribution profile of the normalized photon spectra in the radial distance 0–2 cm given by Brualla et al. 10, 15 & 20 MeV energies from bremsstrahlung yield of x-ray photons have been selected. The 6 MeV has been excluded because it lays below the threshold energies of most reaction channels. The spectral data have been digitized using "GetData Graph Digitizer V2.10" software which represents the photon spectra normalized to one, that assumes the energy integral of flux function is equal to 1:

$$\int_0^{E_{max}} \phi(E)dE = 1 \tag{1}$$

The actual differential flux function $\boldsymbol{\Phi(E)}$, can be calculated by multiplying the normalized differential flux function of the probability density of photon flux count $\boldsymbol{\varphi(E)}$ within energy bin ($\boldsymbol{E}$ to $\boldsymbol{E}+\boldsymbol{dE}$) by the total flux count parameter K.

$$\phi(E) = K \cdot \varphi(E) \tag{2}$$

Fig. 2 illustrates the normalized photon flux rate density for real LINAC of different electron beam energies [8].

The expectation value of mean effective energy over spectrum can be calculated by the following equation:

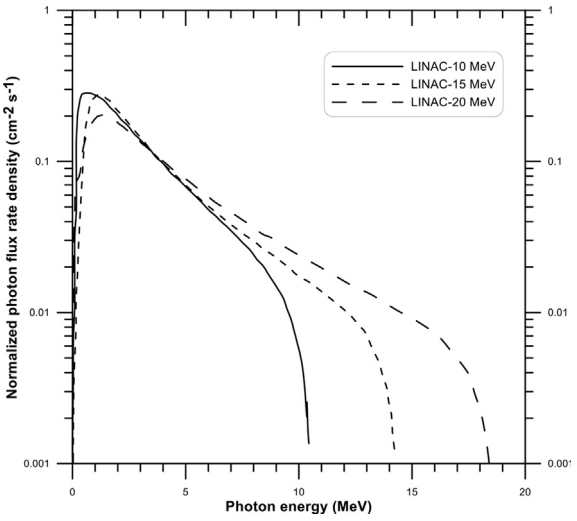

Fig. 2. The normalized of integral of photon flux rate density for different energies of electron beam in clinical linear accelerator, data has been calculated by MC code [14].

$$\overline{E} = \frac{\int_0^{E_{max}} E \cdot \varphi(E)\, dE}{\int_0^{E_{max}} \varphi(E)\, dE} \tag{3}$$

(MATLAB-2012b) was used to calculate $\hat{E}$, the results are as shown in Table 1:

4. Reaction threshold

When a target nucleus X is bombarded by a particles with energy E_a, a compound nucleus (Y) usually in an excited state (Y*) results, which de-excites to Z (the product nucleus) and b (the ejected particle) [15].

$$X + a \rightarrow Y^* \rightarrow Z + b$$

If the ejected particle is a gamma photon, the reaction is called capture reaction or fusion, in some cases, the Z and b products are of comparable mass, so the reaction will be called *spallation reaction* or *fission* [16].

When a stationary nucleus is bombarded by a gamma photon of energy E_γ, the threshold energy, the minimum energy for the reaction, must be equal to the sum of the center of mass kinetic energy of

Table 1. Mean effective energy and the energy of peak flux for different electron beam energies of different medical linear accelerators.

Spectrum	Electron beam energy MeV	E_{max} Photon max energy MeV	($\hat{E}$) Mean effective energy MeV	Energy of peak flux MeV
LINAC-10	10	10.5	2.77	0.6
LINAC-15	15	14.2	3.49	1.2
LINAC-20	20	18.4	4.37	1.3

the target nucleus plus the Q-value of reaction, where:

$$E_\gamma = E_{th} = \frac{1}{2}M_t v_t^2 + Q \tag{4}$$

By solving the velocity of the nucleus to the photon energy and substituting in equation (4), the final formula can be written as [17]:

$$E_{th} = |Q|\left\{1 + \frac{|Q|}{1863A}\right\}\ [MeV] \tag{5}$$

where A is the mass number of the stationary nucleus.

5. Reaction cross-section

Reaction cross-section is defined as the probability of a given nuclear reaction to occur. The unit of the cross-section is the barn (b) (1 b is equal to 10^{-24} cm^2).

The values of cross-sections depend on the energy of the bombarding particle and the type of reaction. Cross-section value can be given by the following equation which is an application of the Breit-Wigner formula [18]:

$$\boldsymbol{\sigma}_{a,b}(E) = \frac{\left(\frac{\Gamma}{2}\right)^2}{(E - E_r)^2 + \left(\frac{\Gamma}{2}\right)^2}\left(\frac{E}{E_r}\right)\boldsymbol{\sigma}_r \tag{6}$$

where E is the incident photon energy, E_t reaction threshold energy, E_r is the giant dipole resonance energy, Γ full width at half maximum (FWHM) at resonance, and σ_r is the cross-section at peak of resonance. This equation describes the reaction cross-section for the formation of a particle resonance, intermediate between two other particle states. Γ is also called the width of level, and it is inversely proportional to the lifetime of a given level

$$\Gamma \propto \frac{1}{\tau} \tag{7}$$

The life-time of compound states nuclide $\boldsymbol{\tau}$ is of the order 10^{-15} s. The width of the resonance is greater for lighter nuclei, and the corresponding life time is shorter, but they'd still be much longer than the characteristics lifetime on the nuclear scale of 10^{-22} s. The width at half maximum $\boldsymbol{\Gamma}$ is given approximately by the equation [19]:

$$\Gamma = 20 \cdot A^{-1/3} \qquad [\text{MeV}] \tag{8}$$

The total Giant Dipole Resonance (GDR) cross-section of compound nucleus, the giant resonance energy E_r, and the width at resonance Γ_r are given by the following equations [8,20].

$$\boldsymbol{\sigma}_{GDR}^{tot} = 60(1 + \boldsymbol{\kappa})\frac{NZ}{A}[\boldsymbol{mb.MeV}] \tag{9}$$

$$E_r = 31.2 \cdot A^{(-1/3)} + 20.6 \cdot A^{(-1/6)}[MeV] \tag{10}$$

$$\boldsymbol{\Gamma}_r = 0.0026 \cdot \boldsymbol{E}_r^{1.91}[\mathbf{MeV}] \tag{11}$$

where κ, is correction factor for the pion exchange which is normally equal to 0.2 for medium mass nuclides, Z and N are the proton and neutron numbers, A is the mass number of the nuclide.

6. Nuclear transmutation

The purpose of externally irradiating a long half-life radioactive isotope is to transmute it to another radioisotope that is of short half-life or, in some cases, stable isotope, taking into account that the product nuclides are also affected by the external beam generating new branches of induced nuclides. In addition to the transmute of casing materials to radioactive nuclides that majorly short-lived half-lives.

For a radioactive nucleus that is exposed to external gamma photons of flux density $\boldsymbol{\phi}$, the change rate of the number of nuclides is given by the *Bateman transformation* equation as [21,22]:

$$\begin{aligned}\frac{dN_i}{dt} = {} & \boldsymbol{productionrate} - \boldsymbol{destructionrate} \\ & - \boldsymbol{decayrate}, (\boldsymbol{i} = \boldsymbol{1}, \boldsymbol{2}, \ldots \boldsymbol{n})\end{aligned} \tag{12}$$

so that

$$\begin{aligned}\frac{dN_i}{dt} = {} & \sum_{i \neq j}\left[\left(\boldsymbol{\gamma}_{j\to i}\boldsymbol{\sigma}_{f\to j}\phi + \boldsymbol{b}_{j\to i}\lambda_j + \boldsymbol{\sigma}_{j\to i}\phi\right)N_j\right] \\ & - \left(\boldsymbol{\lambda}_i + \sum_{i \neq j}\boldsymbol{\sigma}_{i\to j} \cdot \phi\right)N_i\end{aligned} \tag{13}$$

where:

N_j the atomic density of the nuclide i [cm^{-3}];
N_j the atomic density of the nuclide j [cm^{-3}];
$\boldsymbol{\sigma}_{f,j}$ the spectrum-integrated microscopic fission cross-section of nuclide j [cm^2];
$\boldsymbol{\sigma}_{j\to i}$ the spectrum-integrated microscopic of transmutation cross-section of reaction $j \to i$ [cm^2];
$\boldsymbol{\lambda}_i$ the decay constant of isotope i [s^{-1}];
$\boldsymbol{\lambda}_j$ the decay constant of isotope j [s^{-1}];
$\boldsymbol{b}_{j\to i}$ the branching ratio for a specific decay of nuclide i from nuclide j;

$\gamma_{j\to i}$ the fractional fission product yield of nuclide i from the fission of nuclide j;
ϕ the spectrum-integrated photon flux [$cm^{-2}s^{-1}$];

The first term of Equation (13) represents the production rate of nuclide i, while the second term represents the destruction rate out of nuclide i including natural decay.

7. Residual of target nuclide

Assuming a pure sample of mass m_i of radioactive substance (for example ^{137}Cs sample of half-life $\lambda_i equals;$ 30.08 years = 9.486 × 10^8 s and density ρ_i = 1.93 g/cm^3), the total number of Cs nuclides in the mass can be calculated by the equation:

$$N_i = \frac{A_{avogadro} \cdot m_i}{Mass\ Number} = 4.3957 \times 10^{21} \cdot m_i\ [\text{Nuclides}]$$

and the density of atoms is:

$$N_i = \frac{A_{avogadro} \cdot \rho_i}{Mass\ Number} = 8.4837 \times 10^{21} \left[\text{Nuclides/cm}^3\right]$$

Thus, no production rate into i^{th} nuclide exists, so equation (13) is reduced to

$$\frac{dN_i}{dt} = -\lambda_i \cdot N_i - \phi \cdot_i \cdot N_i \tag{14}$$

The exact solution of Equation (14) can be done easily as.

$$N_i(t) = N_i(0) \cdot e^{-(\lambda_i + \phi\,\sigma_i)\,t} \tag{15}$$

where $N_i(0)$ is the initial number of nuclides before irradiation.The *induced decay constant* λ_i* can be defined as

$$\lambda_i^* = \lambda_i + \phi\sigma_i \tag{16}$$

Equation (15) becomes.

$$N_i(t) = N_i(0) \cdot e^{-\lambda_i^* t} \tag{17}$$

By taking the natural logarithms for both sides of Equation (15) as follow.

$$ln(N_i(t)) = ln(N_i(0)) - \lambda_i^* t \tag{18}$$

Subtracting the term $ln(N_i(0))$ from both sides of equation (18)

$$ln\left(\frac{N_i(t)}{N_i(0)}\right) = 1 - \lambda_i^* t \tag{19}$$

where the ratio $N_i(t)/N_i(0)$ represents the normalized number of atoms which also indicates the reduction ratio of the sample. Equation (19) is comparable with the linear relation of the form $y = mx + b$, where the intersect represents the number of initial atoms of the target before irradiation (which is normalized to 1), and the slope represents the value of λ_i*, noting t is the real-time difference and measurements taken just before and after irradiation time.

The residual ratio of original nuclei is calculated by subtracting the reduction ratio from 1, hence.

$$Reduction\ ratio = \frac{N_i(t)}{N_i(0)} \tag{20}$$

$$Residual\ ratio = 1 - \frac{N_i(t)}{N_i(0)} \tag{21}$$

8. Production of nuclides

When bombarding a target nucleus by photon or particle, a compound nucleus will be formed, and after a period of relaxation time, an ejected particle or photon will be emitted from that excited nucleus, leaving it in a different element or isotope nucleus depending on the decay type.

When a compound nucleus is formed, it can decay in a variety of ways, each with its own intrinsic probability. Generally, one way dominates more frequent. For example, when the ^{137}Cs nuclide is irradiated with gamma photons, the compound nucleus corresponding to an excited state of ^{137}Cs can decay in at least the following ways:

$$^{137}\text{Cs} + \gamma \longrightarrow {}^{137}\text{Cs}^* \longrightarrow \begin{cases} ^{136}\text{Cs} + \text{n} \\ ^{136}\text{Xe} + \text{p} \\ ^{135}\text{Xe} + \text{np} \\ ^{134}\text{Xe} + \text{t} \\ ^{133}\text{I} + \alpha \\ ^{135}\text{Cs} + 2\text{n} \\ ^{134}\text{Cs} + 3\text{n} \end{cases}$$

The sum of probabilities of these reactions will give the total photo-nuclear reaction cross-section or total photo-absorption reaction cross-section, given by [23].

$$\begin{aligned} \sigma(\gamma, abs) = {} & \sigma(\gamma, sn) + \sigma(\gamma, p) + \sigma(\gamma, 2p) + \ldots \\ & + \sigma(\gamma, d) + \sigma(\gamma, dp) + \ldots \\ & + \sigma(\gamma, t) + \sigma(\gamma, \alpha) + \ldots \end{aligned} \tag{22}$$

where n is neutron, p: proton, d: deuteron ^2H, t: triton ^3H, α: alpha particle ^4He, and F is total fission products (for heavy nuclei).

The first term in the previous equation represents the total photo-neutron cross-section,

which represents the sum of all photo-neutron reactions

$$\sigma(\gamma,sn) = \begin{matrix} \sigma(\gamma,n)+\sigma(\gamma,np)+\sigma(\gamma,2n)+ \\ \sigma(\gamma,2np)+\sigma(\gamma,n2p)+\sigma(\gamma,3n)+ \\ \sigma(\gamma,3np)+\ldots+\sigma(\gamma,F) \end{matrix} \quad (23)$$

where $\sigma(\gamma,F)$ represents the total photo-fission cross-section (frequently dominant in heavy nuclei).

The yield of produced nuclides j of reaction channel $i \rightarrow j$ is given by the convolution integral of photon flux with cross-section over energy spectrum of reaction, as shown in the following equation [24].

$$\overset{*}{Y}_{i\rightarrow j} = \int_{E_{th}}^{E_{\max}} N_i \cdot \phi(E) \cdot \sigma_{i\rightarrow j}(E)\, dE \quad (24)$$

where $\overset{*}{Y}_{i\rightarrow j}$ is the production rate of nuclide j per unit volume per unit time (atom cm^{-3} sec^{-1}), N_i is the number density of target nuclide (atoms. cm^{-3}), $\phi(E)$ is photon flux density at target atoms (photon cm^{-2} sec^{-1}) which is a function of photon energy E (for continuous spectrum via Bremsstrahlung radiation), and $\sigma_{i\rightarrow j}(E)$ is the cross-section of the reaction $i \rightarrow j$ measured in cm^2 (1 b = 10^{-24} cm^2), and also it is an energy dependent.

The total yield of transmuted nuclides into jth nuclide after a period of time t of irradiation can be calculated by taking the integration over time as follows:

$$Y_{i\rightarrow j}(t) = \int \overset{*}{Y}_{i\rightarrow j}\, dt = \int_0^{t_{total}} \int_{E_{th}}^{E_{max}} N_i(t) \cdot \phi(E) \cdot \sigma_{i\rightarrow j}(E)\, dE dt \quad (25)$$

when using a sample material of monotype atoms (i), the incineration rate of the i atoms due to irradiation by an external photon of energy E ($E_{th} < E < E_{max}$) and also the residual atoms of type i are not constant with time, but it changes as a function of current atom density N_i, as described by equation (13):

$$N_i(t) = N_i(0) \cdot e^{-\left(\lambda^*_{i\rightarrow j}\right) t} \quad (26)$$

where

$$\lambda^*_{i\rightarrow j} = \lambda_i + \phi_E\, \sigma_{i\rightarrow j}(E) \quad (27)$$

(for mono-energy gamma).

For multi-discrete energies E_k eq. (27) becomes:

$$\lambda^*_{i\rightarrow j} = \lambda_i + \sum_k \phi_{E_k} \sigma_{i\rightarrow j}(E_k) \quad (28)$$

and for continues energy of different weighted flux (as provided by bremsstrahlung spectrum), the equation will be written as:

$$\lambda^*_{i\rightarrow j} = \lambda_i + \int_{E_{threshold}}^{E_{max}} \phi(E) \sigma_{i\rightarrow j}(E)\, dE \quad (29)$$

The second term of equation (29) represents the *microscopic reaction rate* per unit time per nuclide, which is also called *Bremsstrahlung weighted cross section* and can be denoted by $\mathbf{R}^{BW}_{i\rightarrow j}(E_{th}, E_{max})$ and is written as:

$$\mathbf{R}^{BW}_{i\rightarrow j}(E_{th}, E_{max}) = \int_{E_{threshold}}^{E_{max}} \phi_{BW}(\mathrm{E}) \sigma_{\mathrm{i}\rightarrow \mathrm{j}}(E) dE \quad (30)$$

where:

$\mathbf{R}^{BW}_{i\rightarrow j}(E_{th}, E_{max})$ is the reaction rate of a certain reaction channel $i \rightarrow j$ [sec^{-1}];
$\phi_{BW}(E)$: photon flux density (*Bremsstrahlung distributed*), which represents the number of incident photons within the energy bin (between E and $E + dE$) [cm^{-2} sec^{-1}]; and
$\sigma_{i\rightarrow j}(E)$: is the partial cross section of a single channel of reaction $i \rightarrow j$ measured by [cm^2].

So the total reaction rate of all possible reaction channels and photon energies can be written as:

$$\mathbf{R}^{BW}_{i\rightarrow all}(E_{th}, E_{max}) = \sum_j^{all} \int_{E_{thr(j)}}^{E_{\max}} \phi(E)\, \sigma_{i\rightarrow j}(E)\, dE \quad (31)$$

By substituting Eq. (31) in Eq. (25) one obtains the number of j product nuclei.

$$Y_{i\rightarrow j}(t) = \int_0^{t_{total}} N_i(t)\, \mathbf{R}^{BW}_{i\rightarrow j}(E, E_{th}, E_{max}) dt \quad (32)$$

Since $N_i(t)$ is the residual target nuclide in time t, then the residual of target nuclides during irradiation process is:

$$N_{i\to all}(t) = \mathrm{N_i}(0)\cdot e^{-\left(\lambda_i + \mathrm{R}_{all}^{BW}(E,E_{th},\mathrm{E}_{max})\right)t}$$

So that equation (32) becomes:

$$Y_{i\to j}(t) = \int_0^{t_{total}} N_i(0)\cdot e^{-\left(\lambda_i + \mathrm{R}_{all}^{BW}(E,E_{th},E_{max})\right)\mathrm{t}} \cdot \mathbf{R}_{i\to j}^{BW}(E,E_{th},E_{max})dt \tag{33}$$

by integration, the total yield of the nuclide j (atoms) is obtained:

$$Y_{i\to j}(t) = \frac{N_i(0)\cdot \mathbf{R}_{i\to j}^{BW}(E_{th},E_{max})}{\lambda_i + \mathbf{R}_{all}^{BW}(E_{th},E_{max})}\cdot \left[1 - e^{-\left(\lambda_i + \mathbf{R}_{all}^{BW}(E_{th},E_{max})\right)t}\right] \tag{34}$$

the yield of daughter via natural decay of the target nuclide during the incineration process is:

$$Y_{decay}(t) = \frac{N_i(0)\cdot \lambda_i}{\lambda_i + \mathbf{R}_{all}^{BW}(E_{th},E_{max})}\cdot \left[1 - e^{-\left(\lambda_i + \mathbf{R}_{all}^{BW}(E_{th},E_{max})\right)t}\right] \tag{35}$$

Finally, the residual target nuclide is.

$$N(t)_{Residual} = N_i(0) - Y_{decay}(t) - \sum_j Y_{i\to j}(t) = N_i(0)\cdot e^{-\left(\lambda_i + \mathrm{R}_{all}^{BW}(E,E_{th},E_{max})\right)t} \tag{36}$$

9. Calculations

A computer program was built using MATLAB, version 2012b [25], to find the numerical results of Equations (34)–(36). The calculations were done with the assistance of the cross section data bank from TENDL-2019 web site [26], which is a nuclear data library mainly developed at PSI and the IAEA – Nuclear Data Section, TENDL provides the output cross-section data of the TALYS nuclear model code system for direct use in both basic physics and applications.

Various photon energies of different photon pattern generated by different sources has been taken, i.e. bremsstrahlung spectrum pattern, discrete mono-energy gamma, and laser Compton scattering pattern. Fig. 3 shows the block diagram of the program.

10. Results

The program shown in Fig. 3 was designed for general target nuclide calculations. It was run using ^{137}Cs, the significant dangerous radioactive waste material. Figs. 4–8 shows the effect of various fluxes and energies on the degradation of ^{137}Cs nuclides after periods of 24 h, 30 days and 1 year of irradiation. The vertical axis represents the normalized residual of 1 g target nuclides (^{137}Cs). The number of ^{137}Cs nuclei were effectively reduced with photon flux over 1×10^{19} [cm^{-2}s^{-1}], also the number of target nuclides was reduced by 10% after 24 h irradiation.

It is clear that the optimum photon energy for relatively higher degradation rate is 15 MeV. This result can be seen in Fig. 9, which represents the reduction of target nuclides versus photon energy for different photon flux densities of 1 g of sample after 24 h of irradiation, and the residual was also normalized to one.

Figs. 10–12 show that the use of flux of 10^{12} [cm^{-2} s^{-1}] is not effective in reducing the ^{137}Cs nuclides,

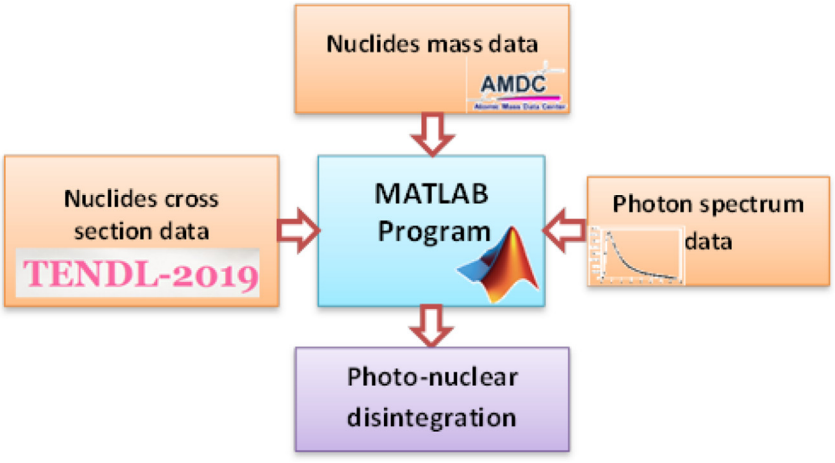

Fig. 3. The block diagram of MATLAB code.

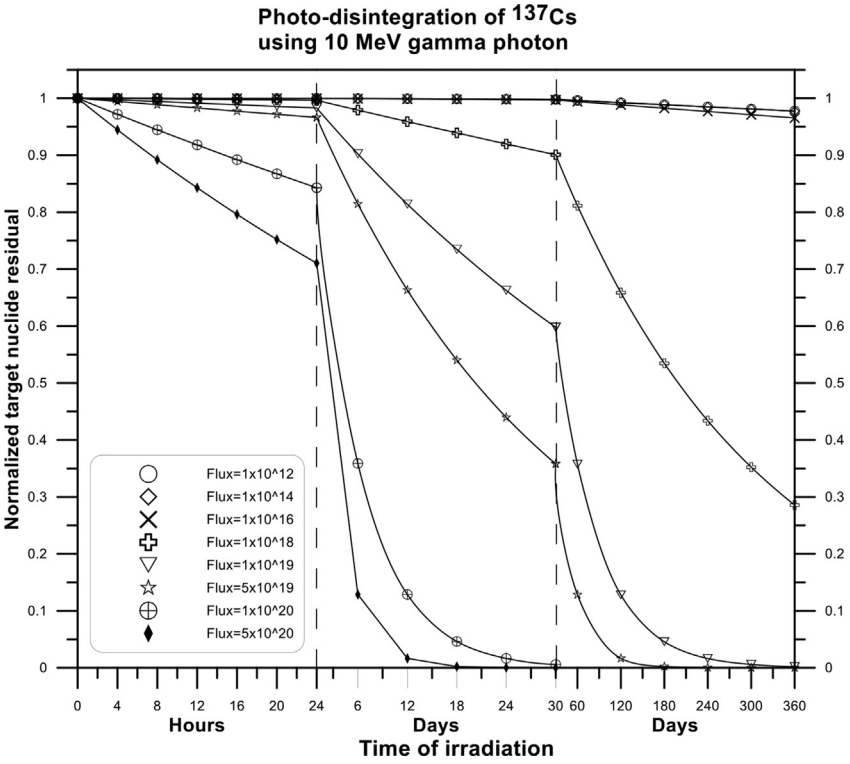

Fig. 4. Residual of photo-disintegration of ^{137}Cs using 10 MeV mono-energy photons.

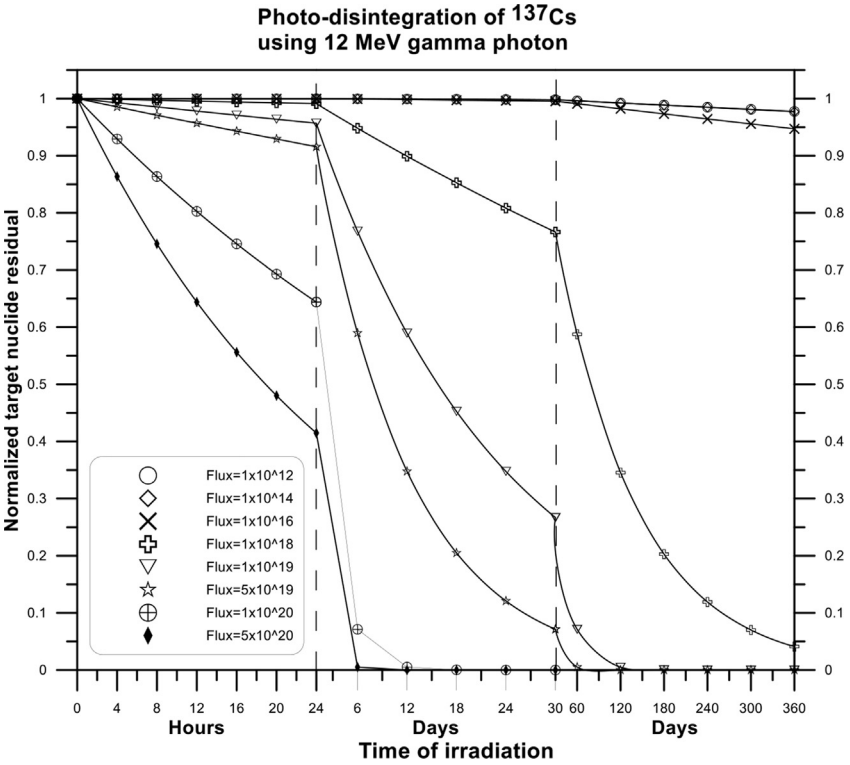

Fig. 5. Residual of photo-disintegration of ^{137}Cs using 12 MeV mono-energy photons.

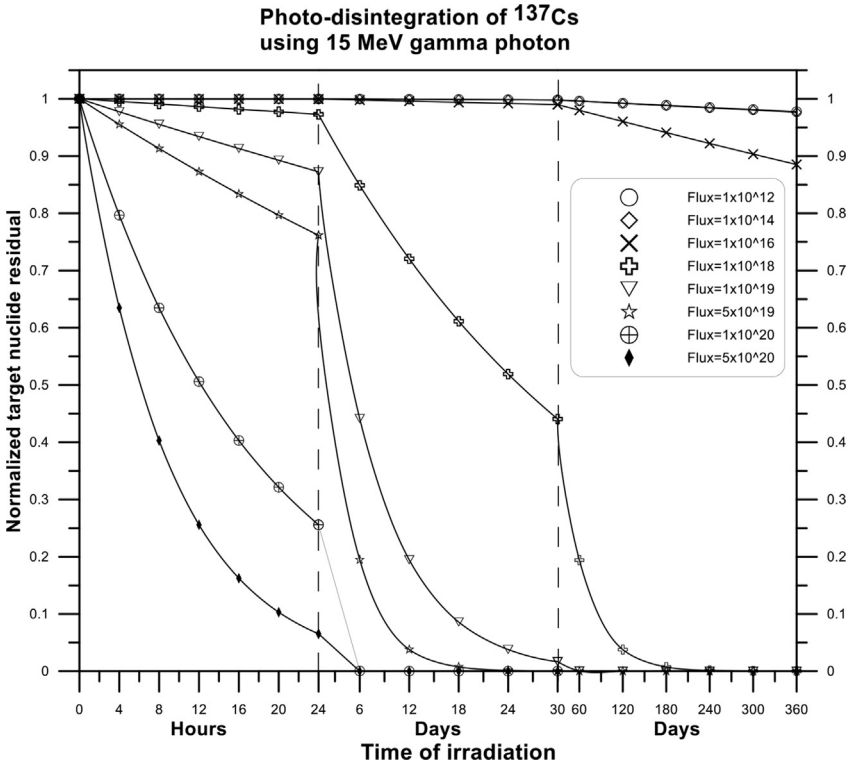

Fig. 6. Residual of photo-disintegration of ^{137}Cs using 15 MeV mono-energy photons.

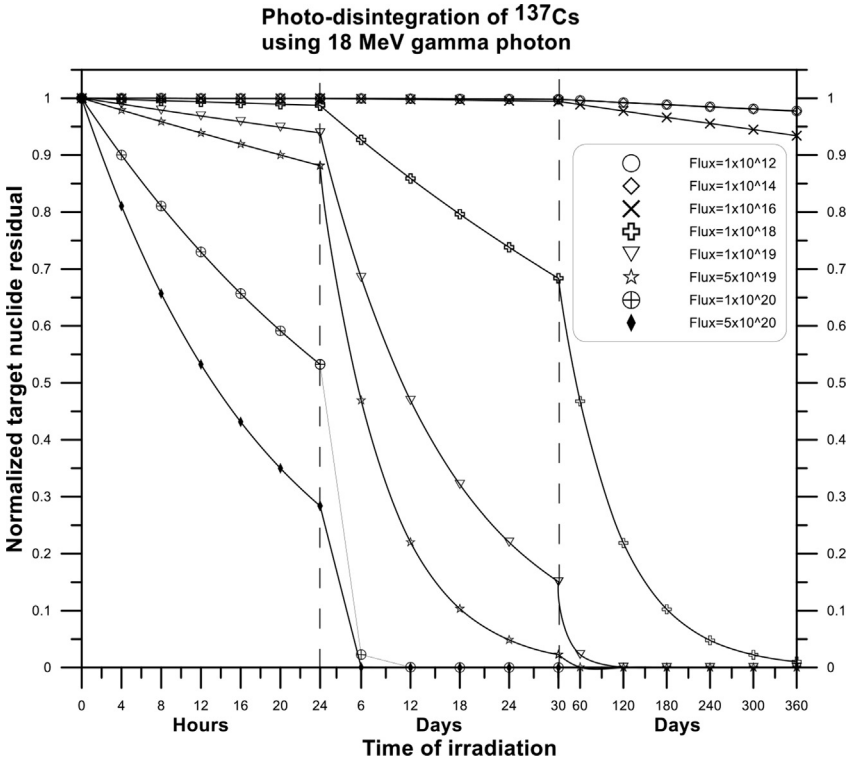

Fig. 7. Residual of photo-disintegration of ^{137}Cs using 18 MeV mono-energy photons.

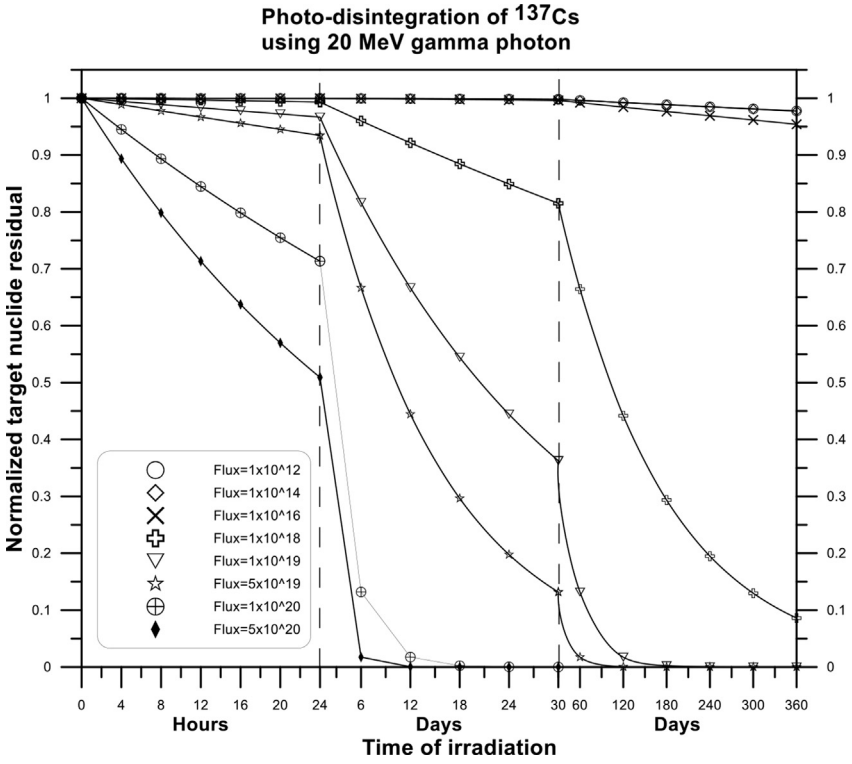

Fig. 8. Residual of photo-disintegration of ^{137}Cs using 20 MeV mono-energy photons.

which means that clinical linear accelerators, which yields maximum photon flux not exceeding 10^{14} photons per cm^2 per second at its best, are not efficient in transmuting radioactive material such as ^{137}Cs nuclide.

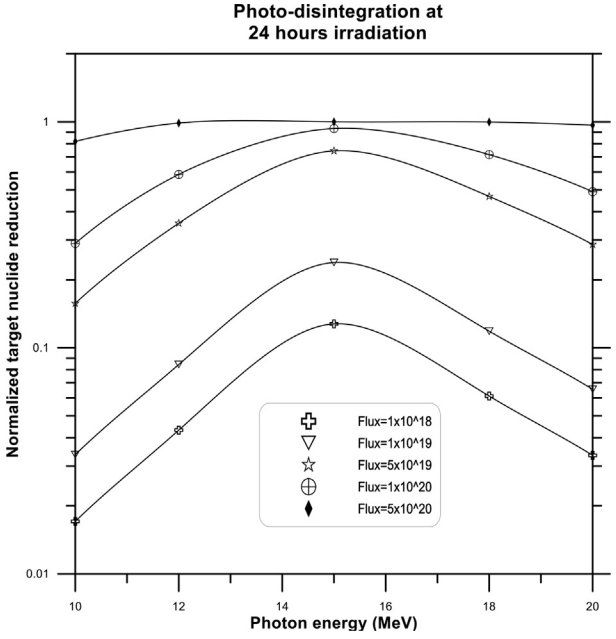

Fig. 9. Reduction ratio of different photon flux density after 24 h irradiation showing the optimum photon energy for best reduction.

For the use of laser Compton scatter (LCS) to generate photon energy of about 15 MeV maximum, it may be assumed to get a flux of gamma photons of about 2×10^{12} photon per second per 500 mA of the electron beam of energy 1.2 GeV that collides with FIR laser of energy 0.7 eV [8]. Although the generated flux is also insufficient to conduct rapid transmutation, the advantages of this method is the high differential flux at the back-end of photon energy spectrum compared with photon flux yield by bremsstrahlung effect of equal maximum energy.

The type of radiation spectrum plays an important role on total incinerated nuclides of ^{137}Cs target. When comparing Fig. 4 with Fig. 10, fig. 6 with Fig. 11 and Fig. 8 with Fig. 12, it was found that the photo-nuclear reaction is higher when the photon flux is concentrated within the region of giant resonance compared with continuous photon spectrum of the same energy yield via bremsstrahlung phenomena and total photon flux.

Table 2 illustrates the most frequent types of reactions channel of gamma photon with ^{137}Cs, the threshold energy to conduct reaction, cross section value at the peak of resonance, corresponding energy to the peak value and the partial width of

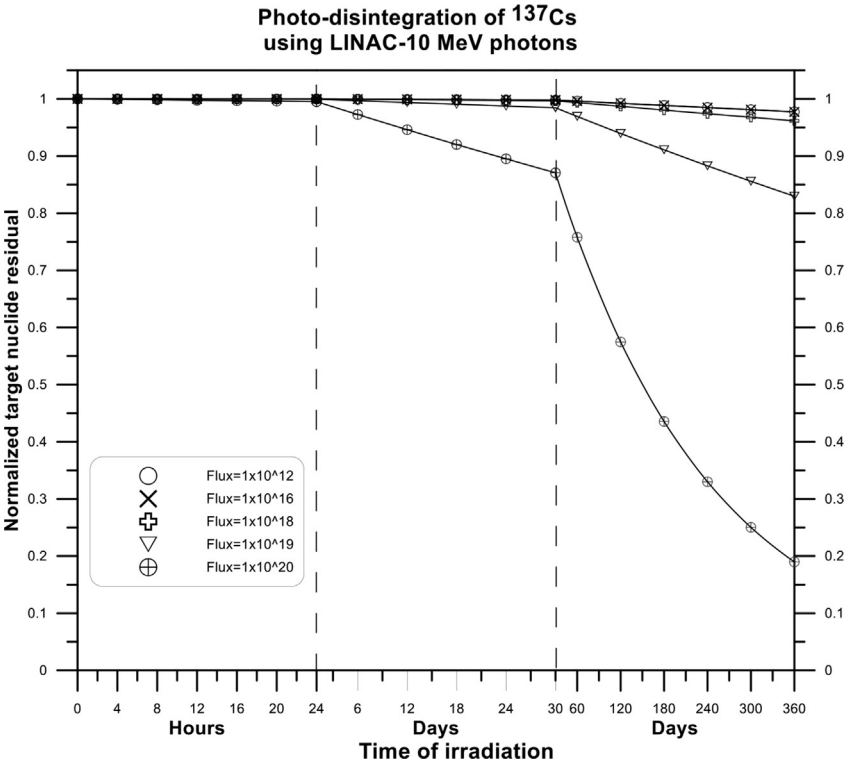

Fig. 10. Residual of photo-disintegration of ^{137}Cs using LINAC-10 MeV photons spectrum.

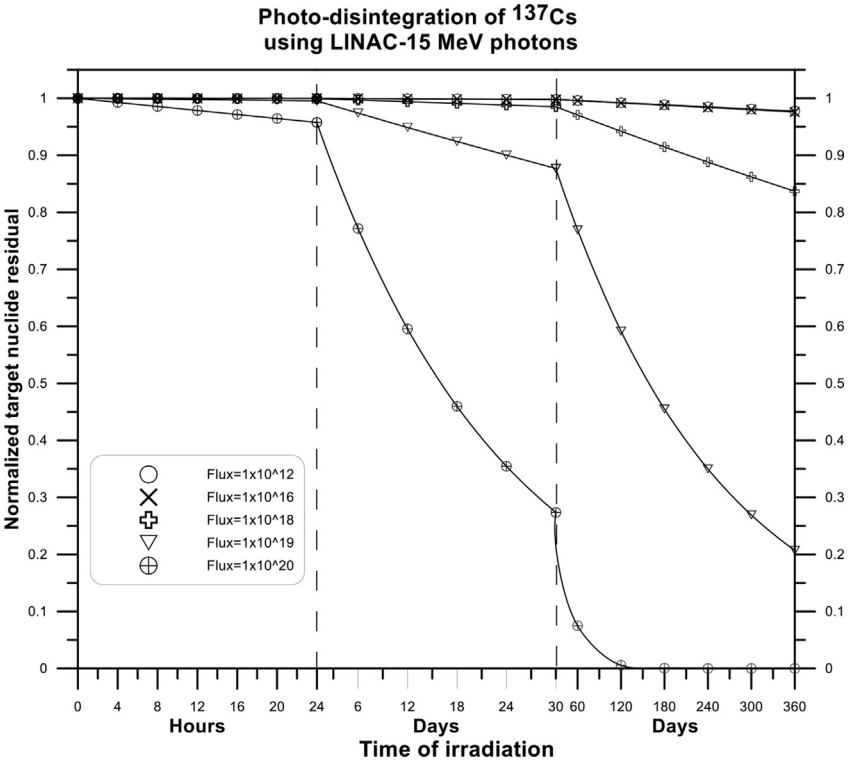

Fig. 11. Residual of photo-disintegration of ^{137}Cs using LINAC-15 MeV photons spectrum.

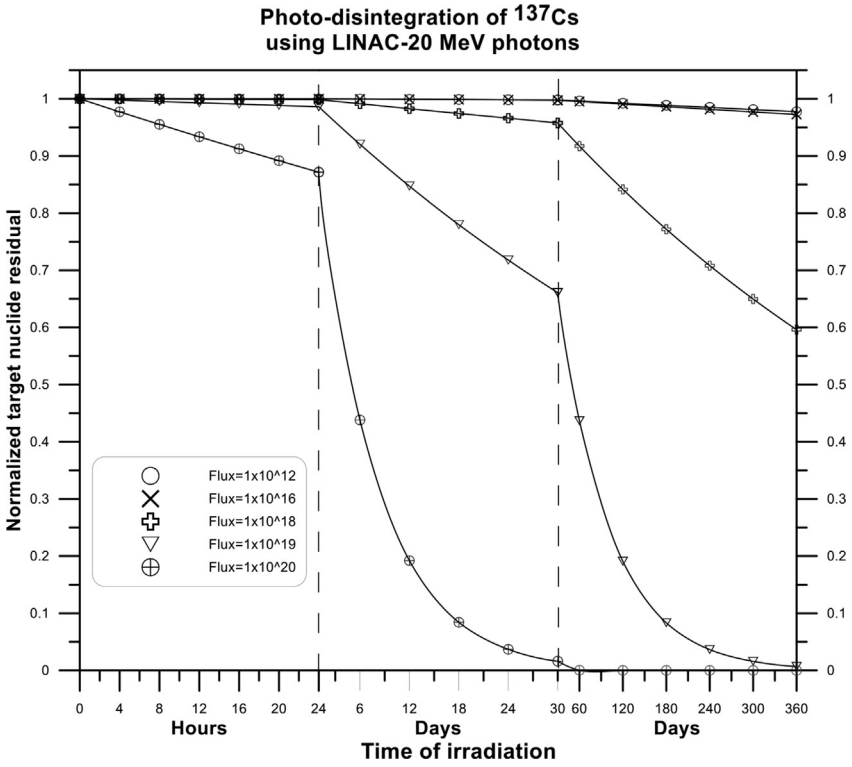

Fig. 12. Residual of photo-disintegration of ^{137}Cs using LINAC-20 MeV photons spectrum.

Table 2. The channels of photo-nuclear reactions of ^{137}Cs sorted from largest cross-section to smallest, threshold of reaction, and energy of giant resonance and partial width.

Reaction channel and products	Half live	Threshold energy (MeV)	Cross section peak σ_{max} (mb)	Energy corresponding to σ_{max} (MeV)	Partial width of reaction Γ (MeV)
^{137}Cs (γ, n) ^{136}Cs	13 d	8.27	324.05	15	3.4
^{137}Cs (γ,2n) ^{135}Cs	2.3×10^{6}y	15.10	116.42	17	4.9
^{137}Cs (γ,3n) ^{134}Cs	2 y	23.87	12.12	30	10.6
^{137}Cs (γ,pn) ^{135}Xe	9.14 h	15.49	0.43	45	97.5
^{137}Cs (γ, p) ^{136}Xe	2×10^{21}y	7.40	0.22	24	17.5
^{137}Cs (γ, d) ^{135}Xe	9.14 h	13.27	1.91×10^{-2}	30	29.5
^{137}Cs (γ, a) ^{133}I	20.8 h	3.11	1.46×10^{-3}	17	9.5
^{137}Cs (γ,2p) ^{135}I	6.6 h	17.34	9.63×10^{-4}	65	63.7
^{137}Cs (γ, t) ^{134}Xe	6×10^{22}y	13.37	3.03×10^{-4}	30	13.9
^{137}Cs (γ,^{3}He) ^{134}I	53 min	17.43	1.12×10^{-5}	45	21.4

Table 3. Shows the time interval of irradiation required to achieve target nuclides reduction to half value from its original amount, note: (y = years, d = days and h = hours).

Total flux cm^{-2} s^{-1}	Photon energy				
	10 MeV	12 MeV	15 MeV	18 MeV	20 MeV
1×10^{12}	30.07 y	30.07 y	30.06 y	30.07 y	30.07 y
1×10^{14}	29.91 y	29.66 y	28.83 y	29.49 y	29.76 y
1×10^{16}	19.51 y	12.56 y	5.65 y	10.03 y	14.53 y
1×10^{18}	199.21 d	78.21 d	25.37 d	54.71 d	101.74 d
5×10^{18}	40.41 d	15.73 d	5.08 d	10.96 d	20.5 d
1×10^{19}	20.25 d	7.87 d	2.54 d	5.49 d	10.26 d
5×10^{19}	4.05 d	1.57 d	12.2 h	1.10 d	2.04 d
1×10^{20}	2.03 d	18.9 h	6.1 h	13.2 h	1.02 d
5×10^{20}	9.73 h	3.78 h	1.21 h	2.61 h	4.9 h

reaction which was computed by measurements of half the width at half maximum in Lorntzian shape of cross section.

From Table 2, it can be seen that some channels need high energy to overcome the threshold and conduct the reaction. Other reactions need relatively low threshold energy, but effective reduction depends on the cross-section of reaction channels. For ^{137}Cs, it is clear from the table that (γ,n) reaction has the largest cross-section followed by (γ,2n)and finally the (γ,3n) reaction, so that the total photo-neutron cross-section is approximately equal to the photo-absorption cross-section of nuclide.

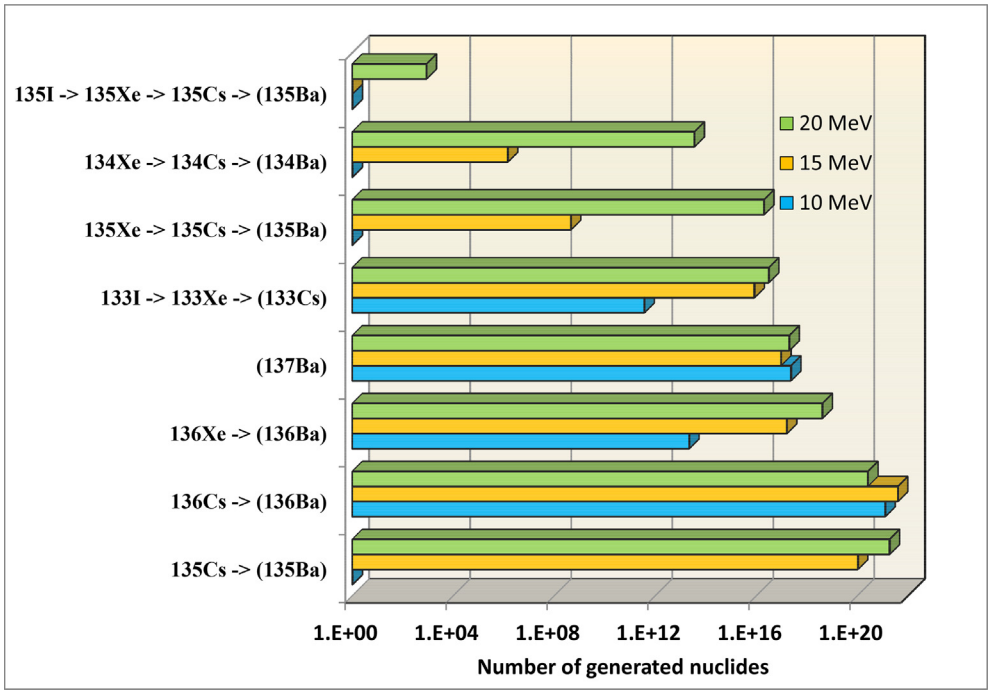

Fig. 13. Produced isotopes as a result of irradiation of 1 gm of ^{137}Cs sample by mono-energetic gamma photons of flux 1 × 10^{20} [$cm^{-2}s^{-1}$] and energy 10,15 & 20 MeV for a period of 24 h.

Some produced nuclides has long half-life such as ^{135}Cs (about 2.3 × 10^6 y) and ^{134}Cs (about 2 y). To avoid production of such isotopes, a softer gamma ray must be used (with energy not exceeding 15 MeV) but a lot of time is needed to give the same reduction ratio. Fig. 12 shows the production rate of the generated nuclides after 24 h of irradiation with flux 1 × 10^{20} [cm^{-2} s^{-1}]. It is clear from the chart that soft gamma ray (of energy below 15 MeV) is better for generating only shorter half-lives nuclides than the use of harder gamma ray.

Table 3 gives a list of the required time intervals of irradiation to achieve target nuclides reduction to half the value of its original amount.

11. Conclusion

By the calculations done on the incineration rate of degradation of ^{137}Cs radioactive nuclides, it is concluded that gamma-ray fluxes (within giant resonance region) lower than 10^{17} [cm^{-2} s^{-1}] are not adequate for performing effective degradation, so that the use of clinical linear accelerators are not effective for transmuting nuclides, and for gamma flux of 10^{18} [cm^{-2} s^{-1}] it was concluded that it provides incineration rate of about 100 times faster than the natural decay of cesium 137.

From Figs. 4–8, it can be concluded that the optimum incineration rate of ^{137}Cs is about the photon energy 15 MeV (for mono-energy gamma) for all flux intensity used, but for continuous spectrum produced by the accelerator, the beam of maximum energy is 20 MeV is better than beams of maximum 10 and 15 MeV.

Finally, the use of gamma energy larger than 15 MeV involves a risk of producing unwanted long-lived radionuclides such as ^{135}Cs (about 2.3 × 10^6 y) and ^{134}Cs (about 2 y) by (γ,2n) and (γ,3n) reactions, so that it is strongly recommended to use gamma photons in the range between thresholds energies of (γ, n) and (γ, 2n) reactions, i.e. the best range of incineration photons E_γ is 8.27<E_γ<15.1 MeV as shown in Fig. 13.

Acknowledgements

The authors would like to thank Prof. Dr. Zainab Al-Sheibani for her valuable comments and revisions.

References

[1] IAEA-safety standard series No. GSG-1, Classification of radioactive waste, IAEA, Vienna, 2009.
[2] IAEA-Technical Document-1817, Selection of technical solutions for management of radioactive waste, IAEA, Vienna, 2017.
[3] K.R. Rao, Radioactive waste: the problem and its management, Curr Sci 81 (12) (2001) 1534–1546.

[4] T. Matsumoto, Calculations of gamma ray incineration of ^{90}Sr and ^{137}Cs, Nucl Instrum Methods Phys Res A268 (1988) 234–243.
[5] B.L. Berman, Atlas of photoneutron cross sections obtained with monoenergetic photons, Atomic Data Nucl Data 15 (1975) 319–390.
[6] W.P. Swanson, Improved calculation of photoneutron yields released by incident electrons, Health Phys 37 (1979) 347–358.
[7] M.A. Saeed, Calculation of (γ − n) Reaction cross-section for radioactive fission products, M.Sc. thesis, University of Baghdad, 2002.
[8] H. Takai, K. Hagino, Nuclear transmutation of long-lived nuclides with laser Compton scattering: quantitative analysis by theoretical approach (Chapter 1), in: K. Nakajima (Ed.), Nuclear back-end and transmutation technology for waste disposal, Springer, Osaka, 2015, pp. 3–11.
[9] R. Kuroda, H. Toyokawa, M. Yasumoto, H. Ikeura-Sekiguchi, M. Koike, K. Yamada, et al., Quasi-monochromatic hard X-ray source via laser Compton scattering and its application, Nucl Instrum Methods Phys Res 637 (2011) S183–S186.
[10] E.B. Podgorsak, Radiation oncology physics: a handbook for teachers and students, IAEA, Vienna, 2005.
[11] R. Mohan, C. Chui, L. Lidofsky, Energy and angular distributions of photons from medical linear accelerators, Med Phys 12 (2) (1985) 592–597.
[12] D. Sheikh-Bagheri, D. Rogers, Monte Carlo calculation of nine megavoltage photon beam spectra using the BEAM code, Med Phys 29 (3) (2002) 391–402.
[13] D. Sheikh-Bagheri, D.W. Rogers, Sensitivity of megavoltage photon beam Monte Carlo simulations to electron beam and other parameters, Med Phys 29 (3) (2002) 379–390.
[14] L. Brualla, M. Rodriguez, J. Sempau, P. Andreo, PENELOPE/PRIMO-calculated photon and electron spectra from clinical accelerators, Radiat Oncol 14 (6) (2019) 1–10.
[15] J. McElhinney, * A.O. Hanson, R.A. Becker, R.B. Duffield, B.C. Diven, Thresholds for several photo-nuclear reactions, Phys Rev 75 (4) (1949) 542–554.
[16] W.E. Meyerhof, Elements of nuclear physics (section 5), McGraw-Hill Education, New York, 1967.
[17] K.H. Beckurts, K. Wirtz, Neutron physics, Springer-Verlag Berlin Heidelberg GmbH, 1964.
[18] E. Hayward, Photonuclear reactions, vol. 118, National Bureau of Standards Monograph, Washington D.C, 1970, pp. 1–43.
[19] A.B. Migdal, A.A. Lushnikov, D.F. Zaretsky, Theory of dipole photoabsorption of nuclei, Nucl Phys 66 (1965) 193–208.
[20] R. Capote, M. Herman, P. Oblozinsky, P.G. Young, S. Goriely, T. Belgya, et al., Nucl Data Sheets 110 (12) (2009) 3107–3214.
[21] J. Cetnar, General solution of Bateman equations for nuclear transmutations, Ann Nucl Energy 33 (2006) 640–645.
[22] J. Cetnar, P. Stanisz, M. Oettingen, Linear chain method for numerical modelling of burnup systems, Energies 14 (6) (2021) 1520.
[23] IAEA-Technical Document-1178, Hand book on photo-nuclear data for applications cross-sections and spectra, IAEA, Vienna, 1999.
[24] M.G. Davydov, G.N. Potetyunko, I.B. Rakhmanov, Calculation of photonuclear reaction yields (scientific and technical reports), Atom Energy 77 (2) (1994) 641–645.
[25] MATLAB R2012b (8.0.0.783), License Number: 874166, MathWorks, Inc. http://www.mathworks.com.
[26] A.J. Koning, D. Rochman, J. Sublet, N. Dzysiuk, M. Fleming, S. van der Marck, TENDL: Complete nuclear data library for innovative nuclear science and technology, Nucl Data Sheets 155 (2019) 1–55, https://doi.org/10.1016/j.nds.2019.01.002.